2.1 Introduction

The conductivity behaviour of the amorphous solid electrolytes or fast ion conducting glasses has been much debated and various models and theories have been developed from time to time regarding their bulk conductivity, relaxational behaviour etc. to reach to a common consensus regarding ion conduction mechanism. In the present chapter, details on general features of ionic conduction in glasses and various theoretical models to understand the conduction mechanisms of ion conduction in glasses have been included. Along with that a discussion on various formalisms of impedance spectroscopy used in the present work has been included in section 2.4.

2.2 General features of superionic conduction in glasses

2.2.1. Cation and Anion Conducting glasses:

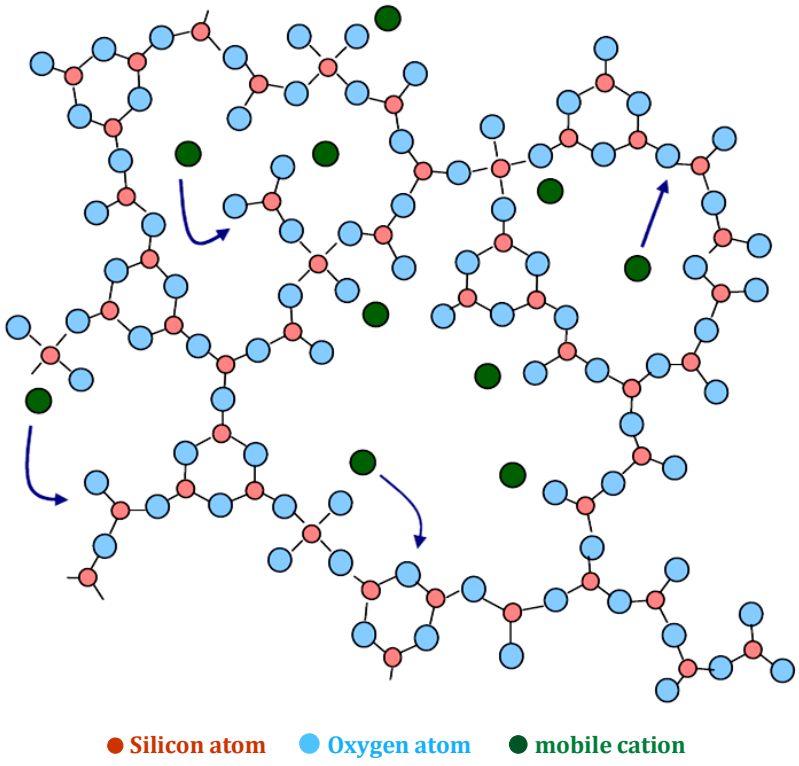

Fig. 2.1. Warren-Biscoe model of the structure of alkali silicate glasses showing motion of cations

The electrolytic properties of an ordinary glass were demonstrated over a century ago by Warburg [1, 2], who electrolyzed Na^+ and other alkali cations through the walls of a thin glass tube and showed that Faraday's laws of conduction were obeyed. The cation mobility (and the corresponding immobility of anions) can be understood intuitively by reference to the widely cited Warren Biscoe version [3] of the structure of alkali silicate glasses (reduced to two dimensions) shown in Fig. 2.1.

According to this simplified picture, cations are placed in "holes" in a glass structure whose shape is largely predetermined by the partially broken (or modified) silicate network. Glasses are thus members of an important class of solid electrolyte materials, which includes fast-ion conductors such as beta-alumina, α-AgI, with cationic transport number, t_+ =1. This form of monopolar conduction is observed in a wide range of borate, phosphate, silicate and molybdate, and many other glasses of varying compositions and stoichiometries.

2.2.2. Effect of temperature on ionic conductivity

It is generally observed that conductivity of a glass rises on increasing its temperature. The dependence of conductivity on temperature can generally be best approximated to the well known Arrhenius equation given as follows,

$$\sigma_{DC} = \sigma_o \exp(-E_\sigma / kT) \qquad \ldots\ldots\ldots (2.1)$$

where, σ_o = conductivity pre-exponential factor, E_σ = conductivity activation energy, k = Boltzmann's constant = 1.38×10^{-23} J/mole-K and T = absolute temperature in Kelvin scale.

2.2.3. The AC Conductivity Spectrum: local motions, long range conduction and Universal power law

Jonscher [4] in his classic paper showed that the AC conductivity data for all material systems, especially in radio frequency regime, can be fit empirically to the following equation.

$$\sigma(\omega) = \sigma_{DC} + A\omega^n \qquad \ldots\ldots\ldots (2.2)$$

where, $\sigma(\omega)$ = AC conductivity, σ_{DC} = DC conductivity, and, $\omega = 2\pi f$ = radial frequency.

This power law behaviour has been observed at such a large scale that it has been termed as the universal behaviour for all ion conducting systems and this empirical relation has been exploited to find out various properties related to ion conduction process like hopping frequency of ions, average relaxation time of ions, DC conductivity etc.

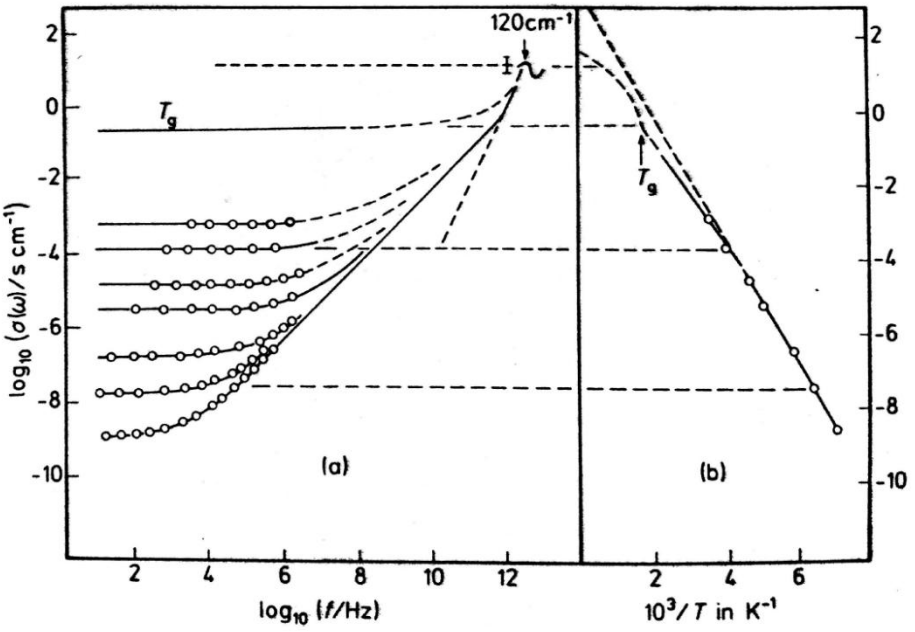

Fig. 2.2. The conductivity spectrum of an AgI-Ag_2O-B_2O_3 glass over a range of temperatures. (From reference [5]).

2.2.4. Near constant loss effects

In many a glass systems, at low temperatures, ac conductivity shows a linear dependence on log *f* with slope = 1. This effect has now been widely accepted to occur in almost all ion conducting glass systems at sub zero temperatures. In the last few decades, ion-conducting glasses (as well as many other solid electrolytes) have been found to show an unexpected degree of similarity in their broadband conductivity spectra. In particular, two surprising universalities' have been detected, (see Fig. 2.2 and Fig. 2.3). One of them, the first universality, has turned out to be a fingerprint of activated hopping along interconnected sites, while the other, the second universality, also known as nearly constant loss (NCL) behaviour, reflects non-activated, strictly localized movements of the ions. The former is observed at sufficiently high temperatures, while the other is found at sufficiently lower temperatures, e.g. in the cryogenic temperature regime.

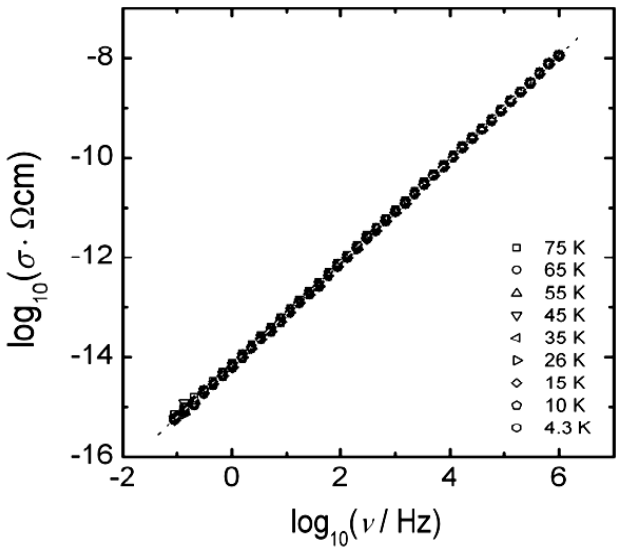

Fig. 2.3. The Second universality (nearly constant loss): Low temperature conductivity isotherms displaying linear frequency dependence and essentially no temperature dependence (Fig. *Taken From* Ref. [6]).

As per Funke *et al.* [7, 8], universal power law and the near constant law, both of them are truly universal and are observable in most ion conducting systems. The fascination of the two universalities lies in their ubiquity, i.e. in the occurrence of either or both of them in quite different kinds of disordered ion-conducting materials [6]. These include crystalline, glassy and polymer electrolytes, molten salts and ionic liquids. Evidently, the existence of the universalities is not primarily a consequence of phase, structure and composition, but rather of some common laws that govern the many-particle dynamics of the mobile ions.

2.3 Theoretical models of superionic conduction in glasses

Ion conduction in solid phase generally involves two aspects (1) Long range migration which is characteristic of DC conductivity and (2) Hopping and relaxation between equivalent sites, and is termed as ac conductivity. Various theoretical approaches taken to understand mechanisms pertaining to ion transport of ion in solid phase/amorphous phase have been proposed by various authors from time to time. Here the main results have been given.

2.3.1. Basic Theory

Total ionic conduction in solid phase may be given as

$$\sigma = \Sigma\, n \cdot q \cdot \mu \qquad \ldots\ldots\ldots (2.3)$$

where, n is charge concentration, q is charge on ion conducting species, μ is mobility of the ion conducting species. It shows that total conductivity is a collective sum of contributions from all mobile species whether, electrons, holes, anions or cations.

2.3.2. The Anderson-Stuart Model

Reported as early as in 1954, it was the very first theory to describe the mechanism of ion conduction in glass materials. The mechanism of ion transport was thoughtfully analyzed in the widely cited model given by Anderson and Stuart [9] in 1954 for Silicate glasses. Conduction is assumed to arise from the hopping of ions between equivalent sites separated by an activation barrier. In this model, the activation energy is comprised of two terms. The electrostatic binding energy of the original site (E_b) and the strain energy (E_s). The binding energy, E_b, describes the Coulombic forces acting on the ion as it moves away from its charge-compensating site, and E_s describes the mechanical forces acting on the ion as it dilates sufficiently the structure to allow the ion to move between the sites. The basic idea is that an ion makes a simple jump from one site to another, and passes through a "doorway" which opens as it passes through, where cation sites require only the presence of the non-bridging oxygens. The model, therefore, estimates the activation barrier E_a as the sum of two terms: $E_a=E_b+E_s$.

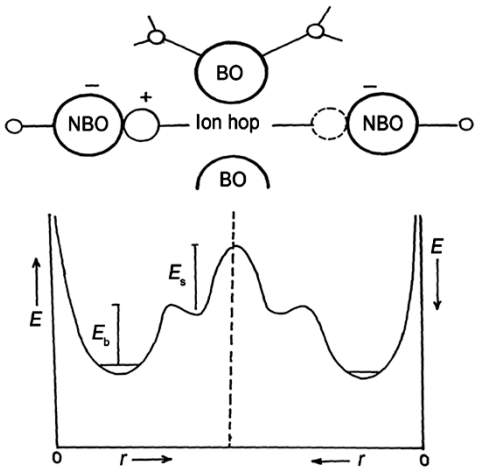

Fig. 2.4. A pictorial view of Anderson-Stuart model.

The A-S model can be expressed as:

$$E_a = \frac{\beta_M}{\gamma}\left(\frac{zz_o e^2}{\delta+\delta_o} - \frac{zz_o e^2}{a/2}\right) + 4\pi G\delta_D\left(\delta-\delta_D\right)^2 \qquad \ldots\ldots\ldots (2.4)$$

where δ and δ_D are the radii of cation and the doorway respectively, a is the jump distance, γ is a covalency parameter arbitrarily taken equal to the relative permittivity ε_r, β_M is the Madelung constant which depends on the spatial arrangement of the ions. z_o and δ_o are the charge and radius of the O^{2-} ion, z is the charge of the cation and G is the elastic modulus. The covalency parameter γ, was seen by Anderson and Stuart as expressing the "deformability of electron clouds on the oxygen atoms". The doorway radius δ_D can be estimated from diffusion data for noble gases such as He, Ne, Ar; since they are uncharged. A simplified version can be derived as the limiting value for $a \to \infty$, we get

$$E_a = \frac{\beta_M}{\gamma}\frac{zz_o e^2}{\delta+\delta_o} + 4\pi G\delta_D\left(\delta-\delta_D\right)^2 \qquad \ldots\ldots\ldots (2.5)$$

During the course of its motion, the ion has to first work against the coulombic interactions, which hold it in its site. Next it has to work its way through a narrow passage known as doorway. Doorway is the opening among the anions which are generally in contact. When three ions are in mutual contact, this doorway is a triangular opening. In oxide glasses like alkali silicates, the doorway oxygens can be a combination of both bridging (BO) and nonbridging (NBO) oxygen atoms. In the A-S model this doorway is assumed to be in the middle of two equivalent ion sites which are well separated. Since the passage of ions require the doorway to be opened, it involves work for pushing the oxygen atoms outwards leading to the compression of atoms in the doorway. This work also contributes to the activation

energy. The model, therefore, estimates the activation barrier E_a as the sum of two terms:

$$E_a = E_b + E_s \qquad \ldots\ldots\ldots (2.6)$$

where, E_b and E_s are electrostatic binding energy and (doorway opening) strain energy respectively. E_b is taken as the difference between the coulombic energy of the carrier ion at the saddle point position - the point of the highest barrier corresponding to the centre of the doorway - and the energy in its own (stable) site.

2.3.3. The Weak Electrolyte Model

According to the weak electrolyte model, which was initially proposed by Ravaine and Souquet [10], liquids or glasses may be considered as weak electrolytes for which the concentration of mobile ions is less than the actual stoichiometric concentration. In this model, the ionic conductivity is expressed as in equation, $\sigma = \Sigma nq\mu$. The weak electrolyte model regards the solvent as a dielectric continuum. Based on this model, conductivity study of Na_2O-SiO_2 glasses [10,11] where network former SiO_2 and the network modifier Na_2O are considered as the solvent and the solute respectively, found a correlation between ionic conductivity and thermodynamic activity of Na_2O (or Na^+) and explained the result by postulating the existence of an equilibrium in the glass.

$$\begin{aligned} Na_2O &\leftrightarrow Na^+ + NaO^- \\ \sigma &= const \times [Na^+] \end{aligned} \qquad \ldots\ldots\ldots (2.7)$$

According to the weak electrolyte theory, the obvious way to improve the conductivity would be to increase the dissociation constant for the equilibrium in equation (2.7). This can be done by choosing a glass network with highly polarizable atoms, which would give a high value of the dielectric constant, ε_r.

2.3.4. Cluster bypass model

Ingram *et al.* [12] proposed a *"cluster bypass"* model to explain ionic conduction in glasses. The basis of the cluster bypass model is the assumption that the liquid phase remains in small regions even far below the glass transition region. These regions of the liquid phase, which decrease in size with decreasing temperature, are situated between clusters of the glassy state. It is supposed that the liquid state forms an interconnected network of pathways, where the cation can diffuse by a percolation process. The decrease in conductivity with decreasing temperature is explained by a decreasing number of favourable pathways as the residual liquid phase progressively solidifies. An advantage of the cluster bypass model is that it may provide a relatively straightforward explanation of the mixed mobile ion effect. The foreign cations are believed to be concentrated in the regions of the liquid phase and there "block" the most favourable pathways. The mobile host cations have to find less favourable pathways involving migration through the glass clusters. This would also explain why the activation energy increases when different cations are mixed.

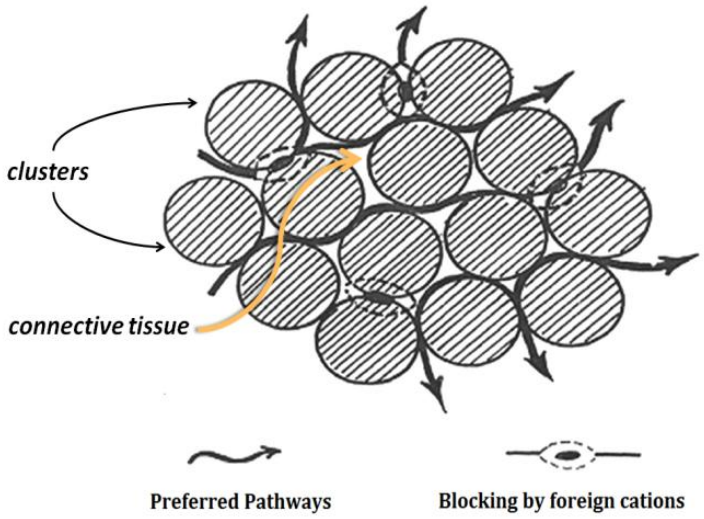

Fig. 2.5. A Schematic of the cluster-bypass model, showing preferred pathways for ion migration located in a connective tissue surrounding microdomains or "clusters" of more densely packed material.

The model recognizes the "cluster-tissue" texture of glasses which was discussed by Burton [13,14] and vitrification was regarded as the congealation (*semi solid nature on freezing*) of ordered microdomains or "clusters" (≫ 50 Å in linear dimension) embedded in a truly amorphous, low density "tissue" material. However regarding the detailed structure of these clusters, Ingram *et al.* [15] have used the model of Goodman [16], according to which the inter-cluster space is filled by a residual liquid which on cooling below T_g solidifies and forms a residual phase or "connective tissue". The central idea of cluster bypass model is that the preferred pathways for ion migration lie within the connective tissue region. The model explains the curvature seen in the Arrhenius plots of certain AgI-rich glasses as due to the continuous exchange of material between the cluster and tissue regions. The authors are able to account for the mixed alkali effect (see later) using this model. Anomalously high dielectric losses in alkali silicate glasses reported by Hyde *et al.* [17]have been attributed in this model to the motion of ions along "partially blocked" pathways. Conductivity enhancements in mixed anion glasses as well as the effects of "dopant" salts such as LiCl have also been explained. NMR studies of sodium silicate glasses have been found to provide supportive evidence to this model [17].

2.3.5. Random Site model

The Random Site Model was proposed by Glass and Nassau [18] in 1980 for Li^+ ion conducting binary glass systems such as Li_2O-B_2O_3, Li_2O-Ga_2O, Li_2O-Al_2O_3 etc. and it proposes that the network modifier or dopant salt is homogenously dispersed in the glass and that its role for the enhanced ion conduction is to lower

the average potential barriers within the glass. The cations are assumed to experience a Gaussian distribution of activation energies due to the randomness of the glass network. The average mobility then varies with the distribution of activation energies and thereby with the glass composition. All the cations are assumed to be potential charge carriers; which means that it is mainly the mobility of the cations which increases with increasing modifier or dopant salt concentration. Therefore, this model is different from the weak electrolyte model, where it is proposed that only a fraction of the cations are mobile and that their mobility is constant.

2.3.6. The Diffusion Pathway Model

The diffusion pathway model [19, 20] was built on the assumption that the metal halide salt is introduced into the amorphous network in small clusters or micro domains, which form connected pathways for the ions to diffuse through the glass. These pathways were assumed to be built up by the halide ions and to be characterized by low energy barriers. While the basic assumption of micro-domain formation cannot be held up, the model remains relevant for network glasses with structures described by the modified continuous random network (CRN) model [11]. This includes metal oxide modified network glasses, where the percolation pathways are formed by inter-network channels of network modifiers and the non-bridging oxygens (NBOs) therein serve a corresponding purpose as the halide ions do for the doped glasses. Thus, the diffusion pathway model shows some similarities with the cluster bypass model, except that the interconnected regions are made up of the dopant salt or the network modifiers, instead of residual liquid in the cluster bypass model.

2.3.7. Jump and relaxation pathways

Proposed by Elliott *et al.* [21], correlated forward-backward hopping sequences of individual mobile charged defects are the elementary process of jump relaxation in solid ionic conductors phenomenon is due to the repulsive interaction between defects. The microscopic dynamics of the relaxation is described in a simple model which yields in particular the frequency spectrum of the hopping motion. With the Help of this function, it is possible to explain the experimental manifestations of the "universal dynamic response", including the well-known arcs in the complex planes of conductivity and permittivity, the power-law frequency dependence of the ionic conductivity, as well as the non BPP-type behaviour of spin-lattice relaxation time and the broad components of elastic neutron scattering results.

2.3.8. The Concept of Mismatch and Relaxation

The Concept of Mismatch and Relaxation (CMR) of Funke *et al.* [22,23] describes the ionic conductivity of disordered materials quantitatively, and explains the frequency-dependent regime (dispersive regime) as a consequence of correlated forward-backward jumps of mobile ions. In the framework of the CMR model, it is assumed that the effective potential on each mobile ion consists of two different parts: a static potential, provided by the immobile glass network, and a time dependent potential, provided by the mobile ions. The jump of an ion to its neighbouring site causes a mismatch to the arrangement of the mobile ions nearby. To reduce this mismatch, either of the neighbours rearranges or the ion jumps back to its original position. This leads to a forward-backward correlation of successive jumps and consequently, to a dispersive regime in the conductivity spectra of ionic

materials. The CMR describes the ion dynamics mathematically by two coupled rate equations. Solid electrolytes with disordered structures, both crystalline and glassy, as well as supercooled ionic melts, exhibit surprisingly similar features in their conductivity spectra, $\sigma'(\omega)$. This finding suggests that the dynamics of the mobile ions in the different systems should be governed by similar rules. Examples are given in this study, including new results on γ-$RbAg_4I_5$, β-AgI, and several glassy electrolytes. In spite of their overall similarity, however, the spectra also display characteristic differences in their shapes and in their scaling behaviour, the latter feature causing, e.g., Arrhenius or non-Arrhenius temperature dependences of the dc conductivity. The observed characteristics of the spectra, both the common and the more specific ones, are well reproduced with the help of two coupled rate equations describing the evolution of the ion dynamics with time. This treatment is based on the jump relaxation model, and is called the concept of mismatch and relaxation (CMR).

$$-\frac{dg(t)}{dt} = A \cdot g^K(t) \cdot W(t) \qquad \ldots\ldots\ldots (2.8)$$

$$-\frac{dW(t)}{dt} = -B \cdot W(t) \cdot \frac{dg(t)}{dt} \qquad \ldots\ldots\ldots (2.9)$$

Here, $W(t)$ is a time-dependent correlation factor, representing the probability for an ion to be still in its new position occupied directly after the jump. It is supposed that a hop of a mobile ion happens at t=0, and hence $W(0)$=1. Furthermore, $W(\infty)$ is the fraction of successful elementary hops. The mismatch function $g(t)$, with $g(0)$=1, describes a normalized distance between the actual position of an ion and the position where its neighbours expect it to be. The parameter A is an internal frequency, proportional to the high frequency limit of the

specific conductivity $\sigma(\infty)$, and B determines the ratio $\sigma(0)/\sigma(\infty) = exp(-B)$. Finally, the parameter K influences the shape of the conductivity spectra in the vicinity of the onset of the dispersion regime and is typically close to 2.

2.4 Impedance Spectroscopy and its various formalisms

To understand electrical properties and charge conduction mechanism, the most straightforward technique is the direct measurement of electrical conductivity by DC methods. However, A particular problem when applying a DC bias to an ionically conducting sample via two standard metal electrodes is polarization effects appearing at the electrodes due to the failure of the mobile ions to traverse the electrolyte/electrode interface (ionic current drops to zero). This difficulty can be overcome by using AC techniques, collectively, called Impedance spectroscopy. AC techniques are more suitable to carry out electrical conductivity studies on ion conducting materials than DC methods.

Impedance spectroscopy is a versatile and established tool to understand various electrical processes like electrochemical reactions, electrode processes, charge transfer processes at electrode-electrolyte interfaces, in materials, electrochemical devices like super-capacitors, fuel cells, batteries, etc. It is a complex yet powerful technique to study and analyze electrical properties of materials, mainly ionic conducting and dielectric ones. Impedance analysis of ionic conducting solids helps in identifying transport properties such total conductivity, ionic transport, grain boundary conduction (for crystalline compositions), electrode-electrolyte interface processes, and relaxation processes etc. It is a non-destructive technique and also can provide the dynamic properties to understand the microscopic nature of the conduction mechanism in superionic conducting materials.

In a general impedance spectroscopy experiment, an electrical stimulus (a known voltage or current) to the electrodes of the specimen is applied and the response is measured. Measurement of the phase difference and the amplitude (i.e. the impedance) allows analysis of the electrode process relating to contributions from diffusion, kinetics, double layer capacitance, coupled homogeneous reactions, etc. It is widely applied in studies of ionic solids, solid electrolytes, conducting polymers, corrosion, membranes and liquid/liquid interfaces [24]. Electrical measurement to evaluate the electrochemical behavior of electrode/electrolyte materials, two identical electrodes applied to the faces of a specimen in the circular form is used. The AC response of the sample to the applied perturbation may be different in phase and amplitude from the applied signal.

2.4.1 Mathematical Foundations of Impedance Spectroscopy

Impedance is generally measured by applying an AC potential to an electrochemical cell. Assume that a sinusoidal potential:

$$V(t) = V_o\, e^{i\omega t} \qquad \text{..... (2.10)}$$

is applied, then the alternating current corresponding to it can be expressed as follows

$$I(t) = I_o\, e^{i(\omega t-\phi)} \qquad \text{..... (2.11)}$$

And the complex impedance can be determined from the equation

$$Z^*(\omega) = \frac{V(t)}{I(t)} = Z_o e^{-i\phi} = Z_o\left(\cos\phi - i\sin\phi\right) \qquad \text{..... (2.12)}$$

where, ω is the radial frequency and ϕ is the phase difference occurring between applied *V(t)* & output *I(t)*

and $$Z_o = |Z| = \sqrt{Z'^2 + Z''^2} \qquad \text{..... (2.13)}$$

The obtained complex impedance $Z^*(\omega)$ can be resolved into its real and imaginary parts as follows

$$Z^*(\omega) = Z'(\omega) - i\,Z''(\omega) \qquad \ldots\ldots\ldots (2.14)$$

Comparing the eq.(2.12) and eq.(2.14), one gets the real and imaginary parts of $Z^*(\omega)$ as follows.

$$Z' = |Z| \cos\phi \qquad \ldots\ldots\ldots (2.15)$$

$$Z'' = |Z| \sin\phi \qquad \ldots\ldots\ldots (2.16)$$

where, Z' and Z'' are real and imaginary parts of the complex impedance $Z^*(\omega)$. In a real impedance spectroscopy experiment, a test signal of fixed voltage level with a sequence of frequencies is applied, and the corresponding impedance, $|Z|$, and phase shift, ϕ, is measured at each frequency. Commercial equipments like Impedance gain-phase analyzers and LCR meters are capable of carrying out such measurements efficiently and accurately with a computerized interface.

Different Formalisms of Impedance Spectroscopy

The ion dynamics can be analyzed using various formalisms of impedance spectroscopy, namely complex impedance $Z^*=Z'(\omega)-iZ''(\omega)$, complex conductivity $\sigma^*=\sigma'(\omega)+i\sigma''(\omega)$, complex dielectric permittivity $\varepsilon^*=\varepsilon'(\omega)-i\varepsilon''(\omega)$ and complex modulus formalism $M^*=M'(\omega)+iM''(\omega)$, where, $\omega=2\pi f$.

All of these formalisms are related to the basic Z^* formalism and are given in the Table 2.1 [25] and have been discussed in detail in forthcoming sections separately.

Table 2.1: Different Formalisms of Impedance Spectroscopy and their inter-relations with complex impedance

	Formalism	Equation	Real and imaginary parts
1.	Impedance	$Z^* = Z' - iZ''$ $Z^* = \|Z\| e^{-i\omega t}$ $Z^* = \|Z\| (\cos\omega t - i\sin\omega t)$ where, $\|Z\| = \sqrt{Z'^2 + Z''^2}$	$Z' = \|Z\| \cos\phi$ $Z'' = \|Z\| \sin\phi$
2.	Admittance	$Y^* = Y' + iY''$ $Y^* = \frac{1}{Z^*}$ $Y^* = \frac{1}{Z' + iZ''}$	$Y' = \left(\frac{Z'}{Z'^2 + Z''^2}\right)$ $Y'' = \left(\frac{Z''}{Z'^2 + Z''^2}\right)$
3.	AC Conductivity	$\sigma^* = \sigma' + i\sigma''$ $\sigma^* = \frac{t}{a}\left(\frac{Z' + iZ''}{Z'^2 + Z''^2}\right)$	$\sigma' = \frac{t}{a}\left(\frac{Z'}{Z'^2 + Z''^2}\right)$ $\sigma'' = \frac{t}{a}\left(\frac{Z''}{Z'^2 + Z''^2}\right)$
4.	Dielectric Permittivity	$\varepsilon^* = \varepsilon' - i\varepsilon''$ $\varepsilon^* = \frac{1}{i\omega C_o} Y^*$ $\varepsilon^* = \frac{1}{i\omega C_o} \cdot \frac{1}{Z^*}$	$\varepsilon' = \frac{-1}{\omega C_o}\left(\frac{Z''}{Z'^2 + Z''^2}\right)$ $\varepsilon'' = \frac{-1}{\omega C_o}\left(\frac{Z'}{Z'^2 + Z''^2}\right)$
5.	Dielectric Modulus	$M^* = M' + iM''$ $M^* = \frac{1}{\varepsilon^*}$ $M^* = i\omega C_o Z^*$ $M^* = i\omega C_o (Z' - iZ'')$	$M' = \omega C_o Z''$ $M'' = \omega C_o Z'$
	where, t = thickness of the specimen a = cross sectional area of the specimen ε_o = permittivity of the free space = 8.85×10^{-12} F/m C_o = geometrical capacitance of the electrodes = $\varepsilon_o (a/t)$		

A thorough treatment of various formalisms of impedance spectroscopy can be found in references like Macdonald [26] and Świergiel [27]. A first observation of these formalisms reveals that all of them can be obtained from the real and imaginary parts of Z^* and are interchangeable. Although all of these formalisms are interchangeable and hence are manifestation of the same microscopic phenomena;

still each of them uniquely identifies various contributions towards charge conduction mechanism. A thorough description on advantages, uniqueness and drawbacks of each of them has been given in the following sections.

2.4.2 Complex Impedance Formalism

The response of a typical ion conductor to an Impedance spectroscopy measurement can be compared to the response of a parallel combination of resistance and capacitor as shown in Fig. 2.9 below, where *R* is the bulk resistance and *C* is bulk capacitance of the specimen.

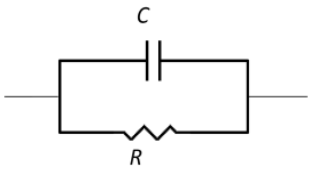

Fig. 2.9. A parallel combination of a Resistance and a capacitance.

Z' and *Z"* in context of the above equivalent circuit containing *R* and *C* can be given as,

$$Z' = \frac{R}{1+(\omega R C)^2} \qquad \ldots\ldots\ldots (2.17)$$

$$Z'' = -\frac{\omega R^2 C}{1+(\omega R C)^2} \qquad \ldots\ldots\ldots (2.18)$$

Now eliminating ω from above equations 2.10 and 2.11, one reaches at the following equation.

$$\left(Z' - \frac{R}{2}\right)^2 + Z''^2 = \left(\frac{R}{2}\right)^2 \qquad \ldots\ldots\ldots (2.19)$$

Equation 2.19 is the equation of a semicircle with radius R/2 and center at (R/2, 0). It shows that the response of the parallel combination of R and C would

result into a regular semicircle intersecting the real axis *Z'* at (R, 0) as shown in the Fig. 2.10 below. It is called the Nyquist plot or the complex impedance plot.

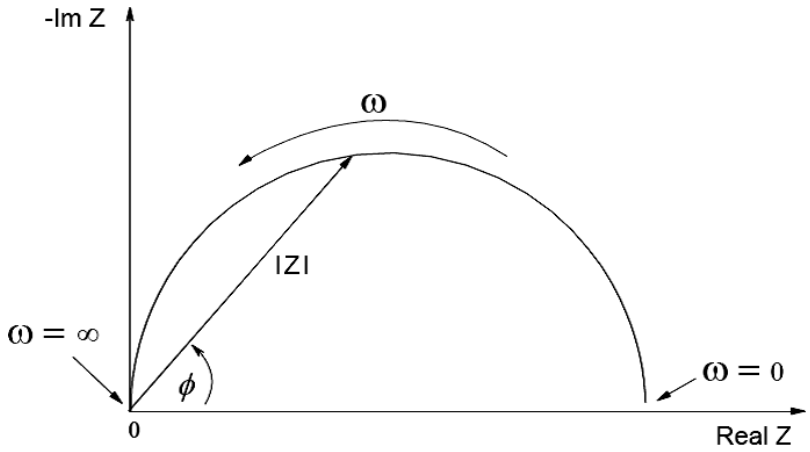

Fig. 2.10. A typical impedance plane plot showing different parameters

It should be noted that in the Nyquist plot of impedance spectroscopy data, each point corresponds to the impedance at one specific frequency; low frequency data are on the right-hand side, while those of higher frequencies are on the left-hand side of the plot.

For a glassy solid electrolyte, a typical Nyquist plot generally looks like as shown in Fig. 2.11 [28]. It shows a semicircular arc in the high frequency region, followed by a polarization spur or a second semicircular (with a comparatively larger diameter) in the low frequency region. The high frequency arc can be extrapolated (on both sides) to the real axis and the difference between these two intercepts with the real axis is taken as the bulk resistance of the sample specimen. The second semicircular arc or the spur occurs due to polarization of mobile ions at sample/electrode interface at lower frequencies.

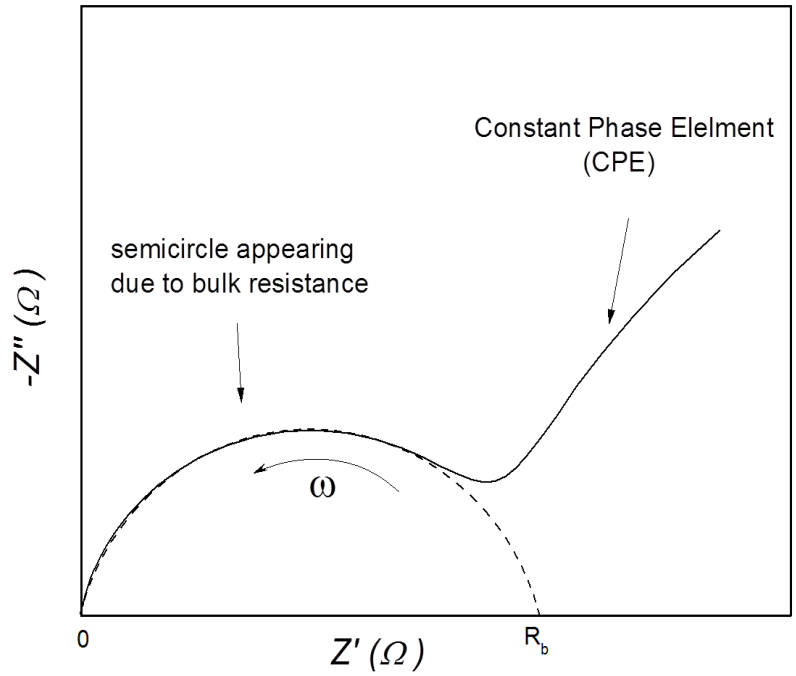

Fig. 2.11. Nyquist plot of impedance for a glassy solid electrolyte with ion non-blocking electrodes.

Equivalent circuit approach to model/understand the impedance response of the superionic conductors under study

The impedance response of superionic conducting materials can be reproduced by very simple electrical circuits having some basic circuit elements like resistance, capacitance, inductance, Warburg and Gerischer elements etc. [29]. The electrical circuit used to re-generate such impedance response is called an "*equivalent circuit*". The complex impedance plots, in general, are modeled using equivalent circuit approach to understand various electrochemical reactions, electrode processes, or ion dynamic processes occurring etc.[29, 30]. However, choice of the equivalent circuit remains in question and sometimes is tricky because a lot of different combinations of resistances, capacitance and other key components like Warburg element, Gerischer element etc. produce the similar impedance responses. However, the equivalent circuit with minimum number of components

should be considered to be the ultimate one and in addition to that its interpretation should be realistic and practicable. For example, the impedance response shown in Fig. 2.10 may be modeled using either of the two equivalent circuits given in Fig. 2.12.

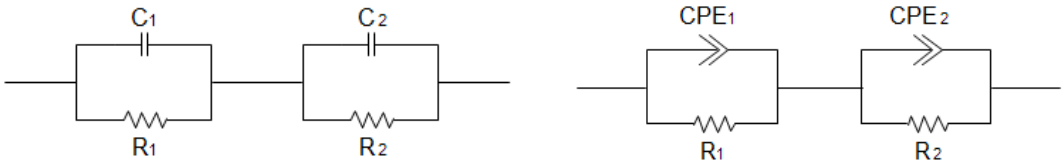

(A) Series combination of two parallel R-C loops **(B) Series combination of two parallel R-CPE loops**

Fig. 2.12. Different Equivalent circuits used to model the impedance response of occurrence of two semicircular arcs in complex impedance plots.

The impedance response presented in Fig. 2.10 can be reproduced either by Series combination of two parallel R-C loops or Series combination of two parallel R-CPE loops, where C is the geometric capacitance between the electrodes, R is the bulk resistance of the sample and CPE is a constant phase element due to the polarization distribution at the interface between blocking electrodes and glass and its impedance can be generally defined using the equation,

$$Z_{CPE} = A(i\omega)^{-\alpha} \qquad \ldots\ldots\ldots (2.20)$$

where, A is an arbitrary constant and α is a constant, usually having values between 0 and 1. With $\alpha = 0$ means it is a purely resistive component and $\alpha = 1$ is attributed to a purely capacitive behavior.

2.4.3 Complex Conductivity Formalism

AC responses of the vitreous solid electrolytes have been widely examined and recently reviewed by Ingram [31]. The first measurement of the frequency-dependent conductivity of Ag^+ conducting vitreous solid electrolytes was reported on the $Ag_7I_4AsO_4$ glass by Grant *et al.* [32], where the Jonscher type [33] frequency dependence of the bulk conductivity was observed.

Complex conductivity may be calculated from the measured complex impedance data conductivity using the following relation,

$$\sigma^*(\omega) = \frac{t}{a}\left(\frac{Z^*(\omega)}{Z'^2 + Z''^2}\right) \qquad \ldots\ldots\ldots (2.21)$$

$$\sigma^*(\omega) = \sigma'(\omega) + i\sigma''(\omega) \qquad \ldots\ldots\ldots (2.22)$$

The real part of σ^* is called AC conductivity, *σ',* and it has extensively been used and analyzed/interpreted by several workers to study/identify various electrical properties of different ion conducting systems like glasses, crystals, polymers, melts etc. [34] . And it can be given as follows from equation 2.20,

$$\sigma' = \frac{t}{a}\left(\frac{Z'}{Z'^2 + Z''^2}\right) \qquad \ldots\ldots\ldots (2.23)$$

AC conductivity spectra are considered to be a universal feature of ion conducting glasses and other disordered systems [35]. Analysis of impedance data using ac conductivity formalism adds a new dimension to the interpretation of relaxation data obtained from the complex impedance measurements.

The frequency response of conductivity in glasses may be entirely due to the translational and localized hopping of ions [36]. The translational hopping gives rise to long range electrical transport at very low frequencies, while the high frequency dispersion may be correlated to the forward-backward hopping of the ions at high frequencies which requires only a fraction of energy that is involved in the long-range diffusion of ions. The frequency independent plateau at low frequency region arises due to contribution of dc conductivity and the switch over of the frequency independent region to frequency dependent region at higher frequencies implies the onset of conductivity relaxation behavior [37], *i.e.* long range migration of ions at low frequencies shifts to short range back and forth hopping between equivalent

sites at higher frequencies and relaxation process starts. Fig. 2.2 shows typical AC conductivity spectra for Ag^+ ion conducting $AgI\text{-}Ag_2O\text{-}B_2O_3$ glass system.

The plateau in the low frequency region occurring before high frequency dispersion may be extrapolated to find out the σ_{DC} value. These frequency dependent conductivity spectra can be best fitted to the well-known Jonscher's universal power law [38],

$$\sigma'(\omega) = \sigma_o + A\,\omega^n \qquad \ldots\ldots\ldots (2.24)$$

where, σ_o is the bulk conductivity, A is an arbitrary constant, ω is the radial frequency and n is a constant called the frequency exponent and its value is generally between 0 and 1. (usually $0 < n < 1$).

2.4.4 Complex Dielectric Formalism

Dielectric formalism of impedance spectroscopy has been traditionally applied to investigate dipolar relaxation in liquids and solids where reorientation of permanent dipoles gives rise to characteristic frequency-dependent features of the complex permittivity [39]. Hence, studying the dielectric properties of an electrically conducting material may seem deceptive, however, as pointed out by Sidebottom *et al.* [40] that in practice, polarization is inseparable from the eventual conduction process. The mobile ion, which creates polarization by reorienting locally, is the same ion that later separates from its immediate neighborhood to produce conduction at lower frequencies. In ion conducting materials polarization and conduction are, therefore, integrated into a single, continuous process. And hence dielectric analysis may shade more lights towards understanding of the ion transport process in ion conducting materials. In an ion conducting system, motion of ions is followed by accumulation of mobile ions at specimen/electrode interface and leads

to polarization of superionic conducting materials [40]. In an ion conducting system, the dielectric constant has contribution from dipoles as well as from mobile ions to the relative permittivity of the materials.

Complex dielectric function along with modulus function and AC conductivity add valuable contribution to understand ion transport mechanism in super ion conducting systems. The complex dielectric function ε^* is given as [41]

$$\varepsilon^*(\omega) = \frac{\sigma^*(\omega)}{i\omega\varepsilon_o} = \varepsilon'(\omega) - i\,\varepsilon''(\omega) \qquad \ldots\ldots\ldots (2.25)$$

where, ε_o is the permittivity of free space and ω is the radial frequency. The real and imaginary parts of ε^* may be separated as follows,

$$\varepsilon' = \frac{-1}{\omega C_o}\left(\frac{Z''}{Z'^2 + Z''^2}\right) \qquad \& \qquad \ldots\ldots\ldots (2.26)$$

$$\varepsilon'' = \frac{1}{\omega C_o}\left(\frac{Z'}{Z'^2 + Z''^2}\right) \qquad \ldots\ldots\ldots (2.27)$$

To study the dielectric properties of prepared glass system, frequency dependent real and imaginary parts of dielectric permittivity are calculated and analyzed using equation (2.26) and (2.27). For this, real *(ε')* and imaginary *(ε")* parts of permittivity as function of frequency at different temperatures are plotted and analyzed further. The real part, ε' is considered to be the true dielectric constant or dielectric permittivity and the imaginary part, ε'' is considered to be occurring due to losses that are inhibited by motion of mobile cations and is generally termed as dielectric loss.

For an ideal Debye type system, $\varepsilon'(\omega)$ spectra exhibit a step-like change from low to high frequency with two plateau regions in lower and higher frequency regions designated as ε_s and ε_∞ respectively, where, ε_∞ is the high frequency permittivity value determined from the $\varepsilon'(\omega)$ at sufficiently high frequencies and ε_s is

static dielectric constant, or static permittivity [42]. In ionically conducting solid materials, the difference $\Delta\varepsilon = \varepsilon_s - \varepsilon_\infty$ (the change in the dielectric permittivity) represents dielectric relaxation strength and it is caused by the relaxation of hopping of ions, and its magnitude depends on the ion-ion correlations as well. In other words, the $\Delta\varepsilon$ term results from the relaxation of hopping of ions [43]. In ion conducting glasses, $\Delta\varepsilon$ is believed to be influenced by ionic transport processes. Sidebottom suggested that the hop of an ion between equivalent anionic sites is analogous to the rotation of a permanent dipole and can be approximated to the Debye model of dipolar relaxation. And the permittivity change, $\Delta\varepsilon$, can be given as [43],

$$\Delta\varepsilon = \frac{\gamma N (qd)^2}{3\varepsilon_o kT} \qquad \ldots\ldots\ldots\ldots (2.28)$$

where, N = total mobile-ion concentration, γ = fraction of N ions that are mobile, q = the charge of the mobile ions, d is the distance traversed in a single hop, a resultant of the product *'qd'* is the effective dipole of a hopping ion, k = Boltzmann's constant and T is absolute temperature.

However in a real system, a difficulty occurs while calculating $\Delta\varepsilon$. The prime reason is that ε_∞ can be determined by taking measurements at sufficiently high frequencies, but the real trouble is faced in determining the low frequency ε_s value. It has been discussed in impedance and AC conductivity formalisms (sections 4.2 & 4.5 respectively), that polarization effects become dominant at lower frequencies due to accumulation of mobile ions at electrodes, and it is quite difficult to separate the true static dielectric constant from the polarization effects. To overcome this difficulty a different approach has been taken by Ngai *et al.* [44] to estimate ε_s at low frequencies by utilizing the high frequency ε_∞ values. They introduced the following

expression to calculate ε_s using ε_∞ value (determined at sufficiently high frequencies, when it approaches a constant value)

$$\varepsilon_s = \beta \frac{\Gamma(2/\beta)}{\left[\Gamma(1/\beta)\right]^2} \varepsilon_\infty \qquad \ldots\ldots\ldots\ldots (2.29)$$

where, Γ is the gamma function, ε_∞ is the high frequency permittivity value obtained from the $\varepsilon'(\omega) \rightarrow \log f$ spectra at sufficiently high values as shown in the graph, and β is the stretched exponential constant obtained from the fitting of the dielectric modulus function (***discussed in the next section***). Hence the dielectric relaxation strength (or dielectric change) can be given as

$$\Delta\varepsilon = \left[\beta \frac{\Gamma(2/\beta)}{\left[\Gamma(1/\beta)\right]^2} - 1 \right] \varepsilon_\infty \qquad \ldots\ldots\ldots\ldots (2.30)$$

2.4.5 Complex Modulus analysis

In AC conductivity analysis, polarization effects become dominant at lower frequencies and hence it is extremely difficult to differentiate between polarization effects and relaxation processes. To overcome this, a new formalism called *dielectric modulus formalism* was developed by Macedo *et al.* in early 70s [45]. It is called; 'electric modulus', 'dielectric modulus' 'modulus function' or simply 'modulus' also. The dielectric modulus and dielectric permittivity are related to each other by,

$$\begin{aligned} M^* &= \frac{1}{\varepsilon^*} \\ &= \frac{\varepsilon'}{\varepsilon'^2 + \varepsilon''^2} + i \frac{\varepsilon''}{\varepsilon'^2 + \varepsilon''^2} \qquad \ldots\ldots\ldots (2.31) \\ M^* &= M' + iM'' \end{aligned}$$

If one considers initially the frequency dependence of M^* for a conductor which exhibits a frequency independent relative permittivity, ε_s, and conductivity, σ_{DC}, the equation of dielectric constant may be rewritten as

$$\varepsilon^* = \varepsilon_s - i\frac{\sigma_{DC}}{\omega\varepsilon_o} \qquad \ldots\ldots\ldots (2.32)$$

Now combining above two equations and introducing the additional parameters,

$$\tau_\sigma = \frac{\varepsilon_o\varepsilon_s}{\sigma_o} \;\&\; M_s = \frac{1}{\varepsilon_s} \qquad \ldots\ldots\ldots (2.33)$$

One may write, M^* as follows

$$M^* = M_s\left(\frac{i\omega\tau_\sigma}{1+i\omega\tau_\sigma}\right) \qquad \ldots\ldots\ldots (2.34)$$

$$M^* = M_s\left(\frac{(\omega\tau_\sigma)^2 + i\omega\tau_\sigma}{1+(\omega\tau_\sigma)^2}\right) \qquad \ldots\ldots\ldots (2.35)$$

$$M^* = M' + iM'' \qquad \ldots\ldots\ldots (2.36)$$

In equation 2.34 & 2.35, τ_σ has unit of time and it is termed as '*conductivity relaxation time*' and is equivalent to the ordinary Maxwell relaxation time for an RC circuit and determines the rate at which the electric field, ***E***, decays to zero in a conducting dielectric under the constraint of constant displacement vector, ***D***.

One of the significant features of equation 2.35 is that it is identical in form to the expression used to describe the relaxation of shear modulus of liquids in cases where use of a single relaxation time is sufficient and τ_σ is analogous to the shear relaxation time, τ_g [45].

The main advantage of modulus formalism is that the polarization effects occurring at the electrode-electrolyte interface are suppressed and the true relaxation

behavior is easily distinguished, generally, in form of a single asymmetric peak in the $M'' \rightarrow \log f$ spectra for most material systems.

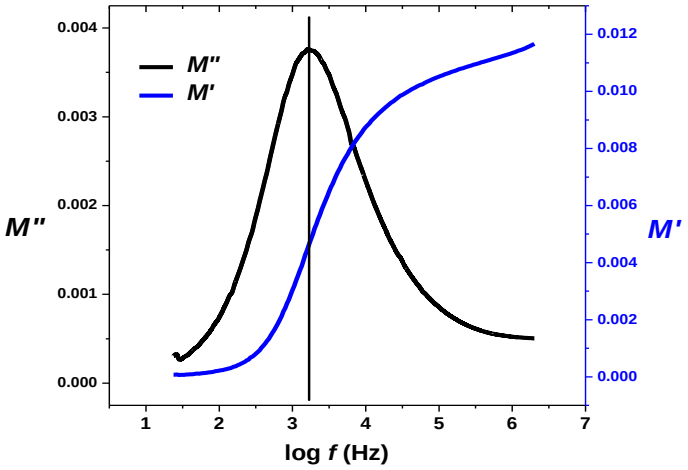

Fig. 2.13. Real and imaginary parts of modulus.

Fig. 2.13 shows typical spectra of real and imaginary parts of modulus for a glass system. It may be noted that M' exhibits a step like increase from low frequency to high frequency region. The tail like "curve" in the low frequency region is devoted to suppression of polarization effects. The M'' spectrum shows presence of an asymmetric peak in the mid frequency region. And it indicates that the relaxation process is of non-Debye type and instead of having a single relaxation time, a distribution of relaxation times prevails.

The frequency corresponding to peak value of M'' is called the characteristics relaxation frequency f_{max}, and is related to the conductivity relaxation time by the following equation, [46, 47],

$$\omega_{max} \cdot \tau_{\sigma} = 1 \qquad \ldots\ldots\ldots (2.37)$$

where, $\omega_{max} = 2\pi f_{max}$.

The frequency range below M''_{max} determines the range where charge carriers are mobile over long distances and contribute to the DC conductivity, whereas in the higher side of the $\omega_{max,}$ the charge carriers are confined to their

potential wells and are able to make hops of short ranges only [48]. Thus, the peak frequency ω_{max} is indicative of transition from long range to short range migration of mobile ions. The consistent shift of the f_{max} position with rise of temperature may be explained on the basis of the distribution of attempt frequencies for the barrier cross-over or a distribution of jumps or flight distances following the cross-over. The broadening of the *M″* versus *log f* curve is interpreted in terms of the distribution of relaxation times for distinguishable processes. According to Hasz *et al.* [49] distribution of relaxation times is connected with a distribution of free energy barriers for ionic jumps, in which, distribution is increased with increasing disorder; whereas Grant *et al.* [50] attributed that distribution of relaxation times is not due to the disordered structure of glasses but is assumed to be the consequence of the cooperative nature of the conduction mechanism (correlated backward-forward hopping of Ag^+ ions).

Further, the *M″* spectra can be best fitted to the stretched exponential *KWW* (Kohlrausch-Williams-Watts) function [51, 52] , using the procedure described by Moynihan *et al.* [53],

$$\phi(t) = \phi_o e^{-\left(\frac{t}{\tau}\right)^{\beta}} \qquad \ldots\ldots\ldots (2.38)$$

where, τ is the characteristic relaxation time and β ($0 < \beta < 1$) is a relaxational parameter representative of distribution of relaxation times and ϕ_o is a constant. The function $\phi(t)$ suggests that the shape of *M″* plot should be asymmetric around the peak and is able to describe the stretched exponential character of relaxation of the electric field.

The exponent β can be evaluated by knowing the *FWHM* (*Full Width at Half Maximum*) of the *M″* plot (frequency axis in log scale), using the relation:

β = (1.14/*FWHM*). It denotes deviation from the ideal Debye behavior. Hodge *et al.* [54] later found that in glasses, higher value of β is related to lower deviation from the ideal Debye behavior. Moreover, value of β is an indicative of ionic conductivity in glasses; higher values of β mean lower ionic conductivity whereas higher ionic conductivity is found to be associated with lower values of β [54].

2.4.6 Electrical Relaxations and the Decoupling Index

Now, as the present system is a class of amorphous solid electrolytes or fast ion conducting glasses, the motion of Ag^+ ions in the glass matrix may be considered to be analogous to their motion in a highly viscous fluid. The Diffusivity of particles in a fluid may be given by the Stokes-Einstein diffusion relation,

$$D = \frac{kT}{6\pi\eta r_i} \qquad \ldots\ldots\ldots (2.39)$$

where, D = diffusivity, η = viscosity , r_i = radius of the particles

Howell *et al.* [55] and afterwards Angell [56, 57] reported that this law does not hold in case of some of molten salts like $Ca(NO_3)$-KNO_3 (*CKN*) and most vitreous solid electrolytes. He further categorized the ionic conducting glass forming materials into two classes: (**1**) the coupled systems: for which the Stokes-Einstein relation holds & (**2**) the decoupled systems: for which this law significantly breaks down. He found that the glass forming vitreous solid electrolytes or super ion conducting glasses belong to the category of decoupled systems. During cooling from melt to glass state, all systems show enormous increase in viscosity (or shear relaxation time), but favorable systems show only a small rise in conductivity relaxation time. Thus, a high conductivity is preserved in the glassy state.

Decoupling of these diffusing particles in the fluid or mobile ions in case of amorphous solids may be represented by the ratio of the average structural

relaxation time τ_s (Tg) to the average conductivity relaxation time τ_σ(Tg) at the glass transition temperature, now popularly called decoupling index,

$$R_\tau = \frac{\tau_s}{\tau_\sigma} \qquad \text{……. (2.40)}$$

Generally τ_S = 200 s at T_g (as it is difficult to determine its value at other temperatures) [58-60], while the τ_σ (Tg) values are determined by extrapolating the $\log\tau_\sigma \rightarrow 1000/T$ plot (Fig.) to T_g of the respective glass samples. Hence we have,

$$R_\tau = \frac{200}{\tau_\sigma} \qquad \text{……. (2.41)}$$

Because this quantity varies between 10^{14} and 10^{-3} for different systems, it is usually sufficient to have approximate values of τ_σ at T_g. Therefore, it is convenient to choose the simple Maxwell relaxation time, an average of a distribution of relaxation time $< \tau_\sigma >$, defined by Macedo *et al.* [61] can be given as,

$$< \tau_\sigma > = \frac{\varepsilon_o \varepsilon_\infty}{\sigma_{DC}} \approx \frac{(9 \pm 5) \times 10^{-13}}{\sigma_{DC}} \qquad \text{……. (2.42)}$$

where, σ_{DC} is the measured conductivity. Hence, combining equations 2.41 & 2.42, decoupling index R_τ, therefore, can be defined simply in terms of the DC conductivity at the reference temperature $T^* = T_g$, as determined by scanning calorimetry at 10˚C/min (T_g = glass transition temperature) [62].

$$R_\tau = \frac{200}{9 \times 10^{-13}} \sigma_{DC} \qquad \text{……. (2.43)}$$

Or,

$$\log R_\tau = 14.3 + \log \sigma_{DC} \qquad \text{……. (2.44)}$$

The conductivity term, σ_{DC}, in equations 2.43 and 2.44 is taken at glass transition temperature by extrapolating the respective Arrhenius plots of σ_{DC} to the glass transition temperature.

References

1. E. Warburg, Wied. Ann. 21 (1884) 63.
2. E. Warburg, Ann. Phys. Chem. 2 (1884) 622.
3. B. Warren, J. Biscoe, J. Amer. Ceram. Soc. 21 (1938) 259 .
4. A.K. Jonscher, Nature 256 (1975) 566.
5. C.A. Angell, Mater. Chem. Phys. 23 (1989) 143.
6. D.M. Laughman, R. D. Banhatti, K. Funke, Phys. Chem. Chem. Phys., 12 (2010) 14102.
7. K. Funke, R.D. Banhatti, I. Ross, D. Wilmer Z. Phys. Chem. 217 (2003) 1245.
8. K. Funke *et al.*, Z. Phys. Chem. 224 (2010) 1891.
9. O.L. Anderson, D.A. Stuart, J. Am. Ceram. Soc. 37 (1954) 573.
10. D. Ravaine, J. L. Souquet, Phys. Chem. Glasses 18(2) (1977) 27.
11. D. Ravaine, J. L. Souquet, Phys. Chem. Glasses 19(5) (1978) 115.
12. M.D. Ingram, M.A. Mackenzie, W. Muller and M. Torge, Solid State Ionics, 28-30 (1988) 677.
13. J.J. Burton, J. Chem. Phys., 52 (1970) 345.
14. J.J. Burton, J. Chem. Phys., 56 (1973) 3133.
15. M.D. Ingram, M.A. Mackenzie, W. Muller, M. Torge, Solid State Ionics 28-30 (1988) 677.
16. C.H.L. Goodman, Phys. Chem. Glasses 26 (1985) 1.
17. J.M. Hyde, M. Tomozawa, M. Yoshiyagawa, Phys. Chem. Glasses 28 (1987) 174.
18. A.M. Glass, K. Nassau, J. Appl. Phys. 51 (1980) 3756.
19. T. Minami, J. Non-Cryst. Solids 73 (1985) 273.
20. G.N. Greaves, J. Non-Cryst. Solids 71 (1985) 203.
21. S.R. Elliott, A.P. Owens, Philos. Mag., B 60 (1989) 777.
22. K. Funke, R.D. Banhatti, S. Brückner, C. Cramer, C. Krieger, A. Mandanici, C. Martini, I. Ross, Phys. Chem. Chem. Phys. 4 (2002) 3155.
23. P. Heitjans, J. Kärger, Diffusion in Condensed Matter, Springer Verlag, Berlin Heidelberg, 2005, p. 857.
24. V.F. Lvovich, Impedance Spectroscopy: Applications To Electrochemical And Dielectric Phenomena, John Wiley & Sons, New Jearsy, 2012.
25. I.M. Hodge, M. Ingram, A. West, J. Electroanal. Chem. 74 (1976) 125.
26. E. Barsoukov, J. R. Macdonald Impedance Spectroscopy: Theory, Experiment, and Applications, Wiley, 2005.
27. J. Świergiel, J. Jadżyn, Ind. Eng. Chem. Res. 50 (2011) 11935.
28. B.V.R. Chowdari, R. Gopalakrishnan, Solid State Ionics 18 -19 (1986) 483.
29. E. Barsoukov, J. Ross Macdonald Impedance Spectroscopy: Theory, Experiment, and Applications, Wiley, 2005.
30. Impedance Spectroscopy: Applications to Electrochemical and Dielectric Phenomena by Vadim F. Lvovich, 2012 John Wiley & Sons, New Jersey.
31. M.D. Ingram, Phys. Chem. Glasses, 28 (1987) 215.

32. R.J. Grant, M.D Ingram, L.D.S Turner, C.A Vincent, J. Phys. Chem. 82 (1978) 2838.
33. A.K. Jonscher, Phys. Stat. Sol. (b) 83 (1977) 585 and 84 (1977) 159.
34. T.B. Schrøder and J. C. Dyre, Rev. Mod. Phys. 72 (2000) 873.
35. A.K. Jonscher, Dielectric Relaxation in Solids, Chelsea Dielectric press, London, 1983.
36. S.H. Chung, K. R. Jeffrey, J. R. Stevens, L. Börjesson, Phys. Rev. B 41(1990) 6154.
37. K. Radhakrishnan, B.V.R. Chowdari, Solid State Ionics 24 (1987) 225.
38. A.K. Jonscher, Nature 267 (1977) 673.
39. K.S. Cole & R.H. Cole, J. Chem. Phys. 9 (1941) 341.
40. D.L. Sidebottom, B. Roling, K. Funke, Phys. Rev. B 63 (2000) 024301.
41. J. Świergiel, J. Jadżyn, J. Phys. Chem. B 116 (2012)3789.
42. H. Froehlich, Theory of Dielectrics, Oxford University Press, Clarendon Press, 1949.
43. D.L. Sidebottom, Reviews in Modern Physics 81 (2009) 999.
44. K.L. Ngai, R.W. Rendell, Phys. Rev. B 61 (1999) 9393.
45. P.B. Macedo, C.T. Moynihan, R. Bose, Phys. Chem. Glass. 13 (1972)171.
46. M. Pant, D K Kanchan, P. Sharma, M.S. Jayswal, Mat. Sci Engg. B 149 (2008) 18.
47. S. Szu, Fu-S. Chang, Solid State Ionics 176 (2005) 2695.
48. J.M. Bobe, J.M. Reau, J. Senegas, M. Poulain, Solid State Ionics 82(1995) 39.
49. W.C. Hasz, C. T. Moynihan, P.A. Tick, J. Non-Cryst. Solids 172-174 (1994) 363.
50. R.J. Grant, M.D. Ingram, L.D.S. Turner, C.A. Vincent, J. Phys. Chem. 82 (26) (1978) 2838.
51. G. Williams, D.C. Watts, Trans. Faraday Soc. 66 (1970) 80.
52. R. Kohlrausch, Ann. Phys. 12 (1847) 393.
53. C.T. Moynihan, L.P. Boesch, N.L. Laberge, Phys. Chem. Glasses 14 (1973) 122.
54. I.M. Hodge, K.L. Ngai, C.T. Moynihan, J. Non-Cryst. Solids, 351 (2005) 104.
55. F.S. Howell, R.A. Bose, P.B. Macedo, C.T. Moynihan, J. Phys. Chem. 78 (1974) 639.
56. C.A. Angell, Solid State Ionics 9&10 (1983) 3.
57. C.A. Angell, Solid State Ionics 18&19 (1986) 72.
58. J. Kawamura, in: T. Sakuma, H. Takahashi (Eds.), Physics of Solid State Ionics, Research Signpost (India), 2006.
59. A. Pan and A. Ghosh, Phys. Rev. B, 62 (2000) 3190.
60. C.A. Angell, Chem. Rev. 90 (1990) 523.
61. P.B. Macedo, C.T. Moynihan, R. Bose, Phys. Chem. Glasses 13 (1972) 171.
62. C.A. Angell, Annu. Rev. Phys. Chem. 43 (1992) 693.